Circadian *per2* regulates the zebrafish central neuronal Mauthner cell axon regeneration via carboxypeptidase E

Dinggang Fan[1]· Keqiang Li[1]· Ziang Zhao[1]· Junhui Zhou[1]· Xiahui Tang[1]· Along Han[1]·Zheng Song[1] Bing Hu[*1]

1. Center for Advanced Interdisciplinary Science and Biomedicine of IHM, Hefei National Research Center for Physical Sciences at the Microscale, Division of Life Sciences and Medicine, University of Science and Technology of China, Hefei 230026, China

Funds:

This work was supported by the core facility Center for Life Sciences, University of Science and Technology of China, Research Funds of the Center for Advanced Interdisciplinary Science and Biomedicine of IHM (QYZD20220002).

Abstract

Central nervous system (CNS) injuries often result in permanent neurological impairments or fatal outcomes. While circadian regulation is a key pathway affecting the regenerative capacity of peripheral neurons, the role of the intrinsic circadian clock in CNS axon regeneration remains elusive. Using a zebrafish larval model with disrupted circadian rhythms, we observed significant inhibition of CNS axon regeneration in a single Mauthner cell (M cell). Mutations or inhibition of the core circadian clock gene *per2* in zebrafish larvae severely impaired axon regeneration and the acoustically evoked escape movements. Time-of-day-dependent transcriptomic analysis revealed that *per2* regulates genes involved in regeneration-related pathways, such

as mitochondrial metabolism and Wnt signaling transduction. Furthermore, quantitative RT- PCR and Western blot experiments indicated that the neurotrophic factor carboxypeptidase E (Cpe) exhibits robust circadian rhythmicity in wild type but is significantly downregulated in *per2*$^{-/-}$ mutants. Cpe deficiency significantly suppressed axonal regeneration, whereas its overexpression enhanced regenerative capacity, thereby rescuing the axonal regeneration impairment in *per2*$^{-/-}$ mutants. Overall, our findings demonstrate the critical role of a stable circadian rhythm system and *per2* in CNS regeneration, as well as the potential function of Cpe in promoting axon regeneration.

Keywords: Circadian clock, Axon regeneration, Zebrafish, Mauthner cells

INTRODUCTION

Injuries to the central nervous system (CNS) profoundly impact neurological functions, positioning them as formidable challenges within neurobiology due to the intricate nature of and difficulties associated with axon regeneration (Varadarajan et al., 2022; Zheng and Tuszynski, 2023). Such injuries often result in irreversible neurological impairments or mortality, underscoring the urgent need for groundbreaking therapeutic approaches. Extensive research has begun to elucidate the mechanisms that either facilitate or impede regenerative processes. For instance, growth factors such as brain-derived neurotrophic factor (BDNF) and nerve growth factor (NGF) have been extensively shown to support neuron survival and axon growth(Allen et al., 2013). In recent years, some novel neurotrophic factors, such as epidermal growth factor (EGF), fibroblast growth factor (FGF), and carboxypeptidase E (CPE), have been discovered, playing protective roles in neuronal survival and growth(Xiao et al., 2017; Cooper et al., 2021). Conversely, extracellular matrix components like chondroitin sulfate proteoglycans (CSPGs) form scar tissue that inhibits regeneration post-injury (Zhai et al.,

2021). Signaling pathways, including mTOR, Wnt/β-catenin, and Notch, play crucial roles in regulating nerve regeneration, while transcription factors such as c-Jun, KLF4, and Sox11, activated during regeneration, regulate gene expression (El Bejjani and Hammarlund, 2012; Fontana et al., 2012; Qin et al., 2013; Sanges et al., 2013; Terenzio et al., 2018; Wang et al., 2015b). Recent research has identified the circadian rhythm as an important factor in peripheral nerve axon regeneration (Halawani et al., 2023). It has been found that circadian axonal regeneration necessitates the neuronal expression of the core circadian clock gene *Bmal1*, which orchestrates the regenerative program of sensory neurons (De Virgiliis et al., 2023). Circadian rhythms, the endogenous oscillations of approximately 24 hours governed by the circadian clock, are pivotal in regulating a myriad of physiological processes, including hormone secretion, cell regeneration, and metabolic pathways (Ruan et al., 2021a; Ruan et al., 2021b). However, the regulation of neuronal regeneration in the CNS by the circadian clock remains elusive.

Zebrafish offer a distinct advantage because they are also diurnal like humans (Appelbaum et al., 2009; Krylov et al., 2021). Furthermore, Mauthner cells (M cells) in the larval zebrafish CNS have emerged as a unique model to study axon regeneration (Hu et al., 2018; Hecker et al., 2020). By injuring one axon and using the uninjured axon as a control, we avoided the impact of cellular heterogeneity, allowing for a more precise investigation into the intrinsic molecular mechanisms of neuronal axon regeneration (Wang et al., 2022; Chen et al., 2024; Shen et al., 2024). Here, we utilized this regenerative model to investigate the regulatory role of circadian rhythms and the circadian clock gene *per2* in axon regeneration. We demonstrated that M cells possess an intrinsic circadian clock. In both juvenile zebrafish models with disrupted

circadian rhythms and in *per2*$^{-/-}$ mutants, axonal regeneration of M cells is significantly impaired, indicating that an intact circadian system is essential for effective regeneration. Transcriptomic analyses conducted over an entire diurnal cycle reveal that the *per2* potentially modulates key regenerative processes such as mitochondrial metabolism and Wnt signaling and concurrently downregulates the expression of the neurotrophic factor *cpe*(Patrón and Zinsmaier, 2016; Wehner et al., 2017). Moreover, single-cell overexpression of *cpe* robustly accelerated axonal regeneration in M cells. These findings not only underscore the critical importance of circadian stability in intrinsic CNS axon regeneration but also reveal that the clock gene *per2* modulates regeneration by rhythmically regulating the expression of the neurotrophic factor *cpe*. This study expands our understanding of the molecular mechanisms underlying CNS regeneration, thereby offering novel approaches for the development of innovative regenerative therapies and the improvement of clinical outcomes in patients with CNS injuries.

MATERIALS AND METHODS

Zebrafish strains and maintenance

The AB wild-type, *per2*$^{-/-}$ mutant (Wang et al., 2015a) and *Tg (Tol-056)* with green fluorescent protein (GFP) tagged M cell were employed. Maintenance of all zebrafish lines was conducted at a constant 28.5°C within an aquatic system subject to a 14:10 light-dark (LD) photoperiod. Embryos, following fertilization, were incubated under equivalent conditions. At 24 hours post-fertilization, pigment formation inhibition was achieved by treating embryos with 0.003% N-phenyl-2-thiourea (PTU, Sigma, USA). Animal care protocols adhered strictly to the ethics guidelines and standards

ratified by the University of Science and Technology of China's Committee on the Ethics of Animal Experiments (approval number USTCACUC 1103013).

Constructing a model of circadian rhythm disruption

Zebrafish embryos were collected 30 minutes post-fertilization and meticulously arranged on sterile glass culture plates. These specimens were then incubated within a hermetically sealed, opaque enclosure, ensuring a complete absence of light until the 6 dpf, establishing the Dark-Dark (DD) cohort. In contrast, the Light-Light (LL) group experienced uninterrupted exposure to light for the same duration. The standard circadian control, known as the LD cycle, consisted of a 14:10 hour light-to-dark ratio. Following the imposition of these environmental conditions, rigorous assays were performed to quantify the expression of circadian rhythm genes and the patterns of locomotor activity within each experimental group, thereby validating the integrity of the induced circadian rhythm disruption model.

Capture the single M-cells in vivo and Single-cell sequencing

Single M-cells were captured in vivo using micropipettes with a tip diameter of approximately 2–3 μm. The cellular contents were aspirated by applying negative pressure and transferred to a PCR tube containing 4 μl of lysis buffer. To minimize contamination, the pipette tip was rinsed 10 times in a 50 mM NaOH solution after capture. Strict RNase-free conditions were maintained throughout the process.

mRNA from individual cells was reverse-transcribed into full-length cDNA using the Smart-seq2 protocol. After quality assessment with an Agilent 2100 Bioanalyzer, sequencing libraries were constructed and paired-end sequencing was performed on an Illumina NovaSeq 6000 platform. Raw reads were preprocessed, aligned to the

zebrafish reference genome (GRCz11) using HISAT2, and gene expression was quantified as TPM values. Downstream analyses included cell scoring based on marker genes, pseudotime trajectory analysis with Monocle, differential expression analysis (|avg_log2FC| > 0.4, p-value < 0.05), and gene set enrichment analysis (Song et al., 2025).

Single-cell electroporation

Precise single-cell electroporation targeting M cell was performed on zebrafish larvae 4 dpf. Before electroporation, the larvae were anesthetized with ethyl 3-aminobenzoic acid ethane sulfonate (MS222, Sigma-Aldrich) and positioned in a custom 1% low melting point agarose mold. A glass microelectrode delivered a 15V, 500-millisecond pulse to electroporate plasmids into the unilateral M-cell. A precision-formed micropipette, created with a pipette puller (Sutter Instrument, USA), was loaded with plasmid solution at 120 ng/μL and placed adjacent to the M-cell soma for electrical stimulation, facilitating the controlled introduction of plasmids into the targeted cell.

Quantitative real time PCR

The total RNA was successfully obtained from the whole larvae utilizing RNAsio (TAKARA). Subsequently, approximately 1 μg of RNA was reverse-transcribed to cDNA through the implementation of HiScript II qRT SuperMix II (Vazyme, China). The RT-qPCR procedure was executed within an overall reaction volume of 10 μL, comprising 5 μL ChamQ Universal SYBR Green qPCR Master Mix and 2 μL cDNA template, deploying the Light Cycler 96 real-time detection system (Roche, China) to surveil and detect significant signal changes. Using the comparative Ct (Cycle threshold) relative quantification method formula $2^{-\Delta\Delta CT}$, mRNA expression levels were

quantitatively evaluated. Notably, the housekeeping gene β-actin mRNA served as an

Table1. Primers designed for cloning and expression analysis in this study

Gene	Gene ID	Note	Forward primer (5'->3')	Reverse primer (5'->3')
β-actin	NC_007112.7	qRT-PCR	ACGAACGACCAACCTAAACTCT	TTAGACAACTAC-CTCCCTTTGC
clock1a	NM_130957.2	qRT-PCR	CTGGAGGATCAGCTGGGTAG	CACACACAGGCACAGA-CACA
per1b	NM_212439.2	qRT-PCR	CCGTCAGTTTCGCTTTTCTC	ATGTGCAGGCTG-TAGATCCC
per2	XM_021478637.1	qRT-PCR	ATGTCGATGGCTTTAGGCAG	CGAGA-CATCCAGAAGGTGCT
per2	XM_021478637.1	mutant identify	AATCCCACGGAAATGAATCTC	CCTTGATGAC-CGTGTTCAAAT
cry2	NC_007136.7	qRT-PCR	ACTATTCAGGAAGAGGCAGAGC	CAGCGGTGGTG-TAGAAGGT
bmal1b	NC_007118.7	qRT-PCR	CCGCATGATCGCAGAAGAAGTG	GGAG-GAGGTGTGCTGTTGGA
per1a	NC_007121.7	qRT-PCR	GGAAAAGGCTCAGCCACAGA	TGAACTTCCGCTCAAAA-GAC
per3	NC_007113.7	qRT-PCR	GTTCTGGCGGAGTAATGGAG	TGACGAC-GTTTTACTGGTGC
aanat2	NC_007114.7	qRT-PCR	CAGGGCAAAGGCTCCATCT	CAGGCAGACAGCG-CAGGT
cpe	NC_007112.7	qRT-PCR	GACCAGAACCGCAACTCACT	GTCGTGGTCGAT-TCCCTCAA
cpe	NC_007112.7	over-ex-pression	GAGCTCCACACGAATTCATGAG GGCGGCGGTGTTTT	CCACCAC-CGCCCATGAATTCGA AGTT-GAGCGTCTCTGACATC
cpe	NC_007112.7	sh-RNA1	AAGGCTTACTCCATCTATAAC	N/A
cpe	NC_007112.7	sh-RNA2	AAGACGGTGACTACTGGCGCT	N/A
cpe	NC_007112.7	sh-RNA3	AACCGCAACTCACTGGTCAAC	N/A

invariant internal control, thereby permitting the normalization of mRNA from target genes. Replication of this process was conducted thrice for each sample to eliminate possible experimental bias and enhance validity. The specific primers utilized in the study are documented in Supplementary Table S1 (Additional file 1).

Drug treatment

The small molecule KL044 (#HY-119506, MCE) has been documented to attenuate Per2 protein activity. Zebrafish larvae were administered KL044 with a terminal concentration of 0.5 μM from 4 dpf until 8 dpf, coinciding with 2 dpi. Similarly, 2-Guanidinoethylmercaptosuccinic acid (GEMSA; #MED18546, Medbio), an inhibitor, was found to decelerate the degradation kinetics of porcine Cpe. For inhibition studies, GEMSA was applied to zebrafish larvae at a final concentration of 50 mM, following the same treatment window from 4 dpf to 8 dpf. Control larvae were exposed to a vehicle solution containing dimethyl sulfoxide (DMSO) and 1-phenyl-2-thiourea (PTU) to mitigate pigmentation and ensure transparent observation of physiological changes.

Protein extraction and western blotting

Each group, encompassing wild-type, *per2*$^{-/-}$ mutant, KL044 and GEMSA inhibitor-treated zebrafish, consisted of 60 larvae. Proteins were extracted using kit (PK10024, Proteintech), ensuring high-quality samples. After boiling and electrophoresis on a 10% SDS-PAGE, proteins transferred to an NC membrane. Post blocking with a protein-free solution (G2052, Servicebio, China), membranes were incubated with primary antibodies against Cpe (Sangon Biotech, China) or Gapdh (HuaAn Biotech, China) at 4 °C overnight. Secondary anti-rabbit antibodies (Proteintech, China) followed for 1 hour at room temperature. After TBST washes, visualization was by ECL system (Thermo Fisher, America). Band intensities were analyzed with Image J and normalized to Gapdh.

Proteomic Analysis of *per2*$^{-/-}$ Mutant Zebrafish

Proteomic analysis was conducted using the Bioprofile mass spectrometry platform (Cox and Mann, 2008; Parker et al., 2015). After grinding samples in liquid nitrogen, SDT lysis buffer was added, followed by incubation in a boiling water bath for 3 min and ultrasonication for 2 min. The lysate was centrifuged at 16,000 × *g* for 20 min at 4 °C, and the supernatant was collected for protein quantification via the BCA assay. Proteins were digested using the FASP method and separated on a Vanquish Neo UHPLC system (Thermo Scientific).Data were processed with DIA-NN for database searching and quantification. Raw DIA files were analyzed using a Q-value ≤ 0.01 as the filtering threshold. Proteins identified in at least 50% of samples within any experimental group were retained; missing values were imputed, and statistical analysis was performed. Proteins with a fold change > 2.0 (up- or down-regulated) and a p-value < 0.05 were considered significantly differentially expressed.

RNA Sequencing and Analysis

Total RNA was extracted using TRIzol, with integrity assessments performed on the Agilent 2100 Bioanalyzer. New England Biolabs' (NEB) standardized protocols facilitated subsequent library construction, with a Qubit 2.0 Fluorometer providing library quantitation. Ensuring normalization to 1.5 ng/μl and validating insert sizes via Bioanalyzer precluded qRT-PCR verification of a minimal 1.5 nM concentration requisite for sequencing. Quality-conforming libraries coalesced, advancing to next-generation sequencing on the Illumina platform. Post-sequencing, CASAVA distilled raw imaging data into sequence reads in FASTQ format, followed by a stringent cleansing regimen that excised adapter sequences and enforced quality and error rate checks.

The HISAT2 aligner proficiently mapped the polished reads to the zebrafish reference genome. String Tie orchestrated transcriptome reconstruction and annotation, interfacing with Pfam and KEGG databases for functional annotations. Read quantification via feature Counts, and differential expression scrutiny by DESeq2 illumined shifts in gene expression. Circadian rhythmimity of gene expression was analyzed with the MetaCycle v1.1.0 R package, employing the meta2d function with parameters (Cyc Method="JTK", timepoints=rep (seq (9, 29, by = 4), each = 2)) calibrated to pinpoint transcripts with a 24-hour expression cycle (De Virgiliis et al., 2023). A minimum expression threshold during MetaCycle evaluation sifted non-expressed genes, bolstering the analysis of circadian gene expression dynamics.

Behavioral test

Locomotor Rhythm Analysis. zebrafish larvae were assessed under constant DD, LL and LD cycles using a Zebrabox system (Viewpoint, France). Experiments were conducted with three groups, comprising wild-type (WT/AB) larvae at 6 dpf, housed in a 48-well plate, with 16 larvae allocated to each experimental condition. Under DD conditions, larvae were exposed exclusively to infrared illumination for three days to maintain an uninterrupted dark environment. Conversely, LD conditions simulated a regular photoperiod, providing light from 8:30 a.m. to 10:30 p.m. for a similar duration.

The VMR experiment is based on the principle that zebrafish larvae exhibit distinct motor responses when exposed to changes in light conditions. Zebrafish have a highly sensitive visual system. In this study, 6-day-old WT/AB and *per2*$^{-/-}$ mutant zebrafish were placed in a 48-well plate and dark-adapted for 2 hours. Afterward, the lights

were suddenly turned on, and the changes in the larvae's motor behavior were recorded for 60 seconds before and after the transition from darkness to light. This visually induced motor response is primarily regulated by the retina and the central nervous system, reflecting the zebrafish's visual perception abilities and neural activity status.

Free swimming. Behavioral tests of free-swimming in zebrafish were performed to test whether zebrafish motor function was affected by gene knockout. The Viewpoint (France) instrument was used to record the free-swimming trajectory of 6 dpf larvae for one hour, and the moving distance was calculated.

Escape behavior assay. The functional recovery of zebrafish M cell was examined by escape response test. The equipment used in this experiment included a high-speed photographic camera (1000 fps, Revealer, China), a sound source (produce 500 Hz, 20 ms sound stimulation), a lighting platform and a computer. Escape responses were tested on zebrafish larvae at 8 dpf which were placed in 60 mm diameter petri dishes containing EM solution. High-speed photographic cameras, adjusted to the suitable focal length, were employed to capture the responses. A computer-controlled the acoustic stimulus and recorded the process of the escape response. The videos were analyzed with professional software (Revealer, China) to record the maximum turn of larvae and the time required to reach the maximum turn when the escape response occurred.

The Viewpoint system, enclosed in an incubation chamber regulated at 28.5°C, facilitated continuous behavioral tracking. Locomotor activity was meticulously recorded for two consecutive days using the integrated video tracking capability of the Zebrabox and data collated through the Zebralab 3.11 software (Viewpoint, France).

Statistical analysis

Graphical representations and statistical significance were evaluated using GraphPad Prism version 10.0 (San Diego, USA), alongside Adobe Photoshop CC 2021 and Adobe Illustrator CC 2021 for figure preparation. Quantitative data are expressed as mean ± standard error of the mean (SEM). Comparative analyses were performed employing unpaired two-tailed Student's *t*-tests for two-group comparisons. For experiments with more than two groups, one-way analysis of variance (ANOVA) was conducted, while two-way ANOVA was applied to assess the effects of two independent variables. Each experiment was replicated a minimum of three times to ensure reliability. Statistical significance was ascribed at * $p < 0.05$, ** $p < 0.01$, *** $p < 0.001$, and **** $p < 0.0001$. Detailed methodological particulars, including sample sizes and the specific statistical tests implemented, are elucidated in the figure legends.

RESULTS

Disruption of the circadian rhythm significantly inhibits the axon regeneration capacity of M cells

Clock/Bmal activation of Per/Cry transcription and periodic self-inhibition establishes circadian oscillation (Huang et al., 2016). Studies have demonstrated that five to six light-dark cycles were required for zebrafish embryos to establish stable biological rhythms (Chen et al., 2023). To investigate the effects of circadian rhythms on the axon regeneration capabilities of CNS, particularly M cells, we established a zebrafish model of circadian rhythm disruption by keeping embryos under various lighting conditions—normal light/dark (LD; 14 hours light:10 hours dark), constant darkness (DD), and constant light (LL) for six days **(Figure 1A, B)**. To assess the expression of core circadian clock genes, quantitative real-time PCR results showed a significant

disruption of the rhythmic expression of the *clock1a* and *per2* genes, and a reduced rhythmic amplitude of the *bmal1b* and *cry2* in larvae zebrafish reared under LL and DD conditions (**Figure 1C,1D and Supplementary file 2**). Although circadian rhythm genes are present in nearly all cells of an organism, to confirm the presence of an endogenous molecular clock in M cells, we targeted M cells *in vivo* from 6 dpf (days post fertilization) *Tg (Tol-056)* zebrafish (**Figure S1A, S1B**) and assessed the integrity of their cDNA library using the Agilent 2100 Bioanalyzer (**Figure S1C**). Subsequent quantitative PCR analysis of core circadian clock genes, including *clock1a*, *bmal1b*, *per1b*, *cry2*, and *per2*, demonstrated the abundant expression of circadian clock genes in M cells (**Figure S1D**). Sleep is a behavioral output reflecting the stability of the circadian clock (Lane et al., 2023). Behavioral assays revealed that the peaks and troughs of locomotor activity were absent in larvae reared under LL and DD conditions compared to those under the LD normal conditions, indicating a disruption of sleep activity rhythms (**Figure 1E–1G**). These data suggest that the circadian rhythms of zebrafish reared under DD and LL conditions were severely disordered.

M cells, a pair of motor neurons located in the zebrafish hindbrain, with a soma diameter of up to 50 μm in diameter and an approximately 2800 μm long axon, extend through the entire spinal cord are stably labelled in the transgenic line *Tg (Tol-056)* (**Figure 1H**)(Korn and Faber, 2005; Sillar, 2009). To exclude the impact of circadian rhythm disruption on the development of M cells, the soma and axon lengths from the injury site (just above the cloacal pore) to the tail were measured in 6 dpf zebrafish reared under LD, LL, and DD conditions (**Figure S2A, S2F**), but no significant differences were found (**Figure S2C, S2D**). Similarly, the whole-body length of 6 dpf zebrafish, showed no significant changes under these three conditions as well (**Figure**

S1B, S1E). Subsequently, Axonal ablation was performed directly above the cloaca with a two-photon laser. As expected, the injured axon exhibited noticeable ablation and degradation within a few minutes post-injury. Two days post-injury (dpi), axonal regeneration was imaged **(Figure 1I)**. Larval zebrafish with disrupted circadian rhythms showed a significant length reduction of the regenerated axons **(Figures 1J, 1K)**. These results indicated that circadian rhythms played a regulatory role in the process of M cells axonal regeneration, and disruptions in these rhythms impaired axonal regenerative capabilities.

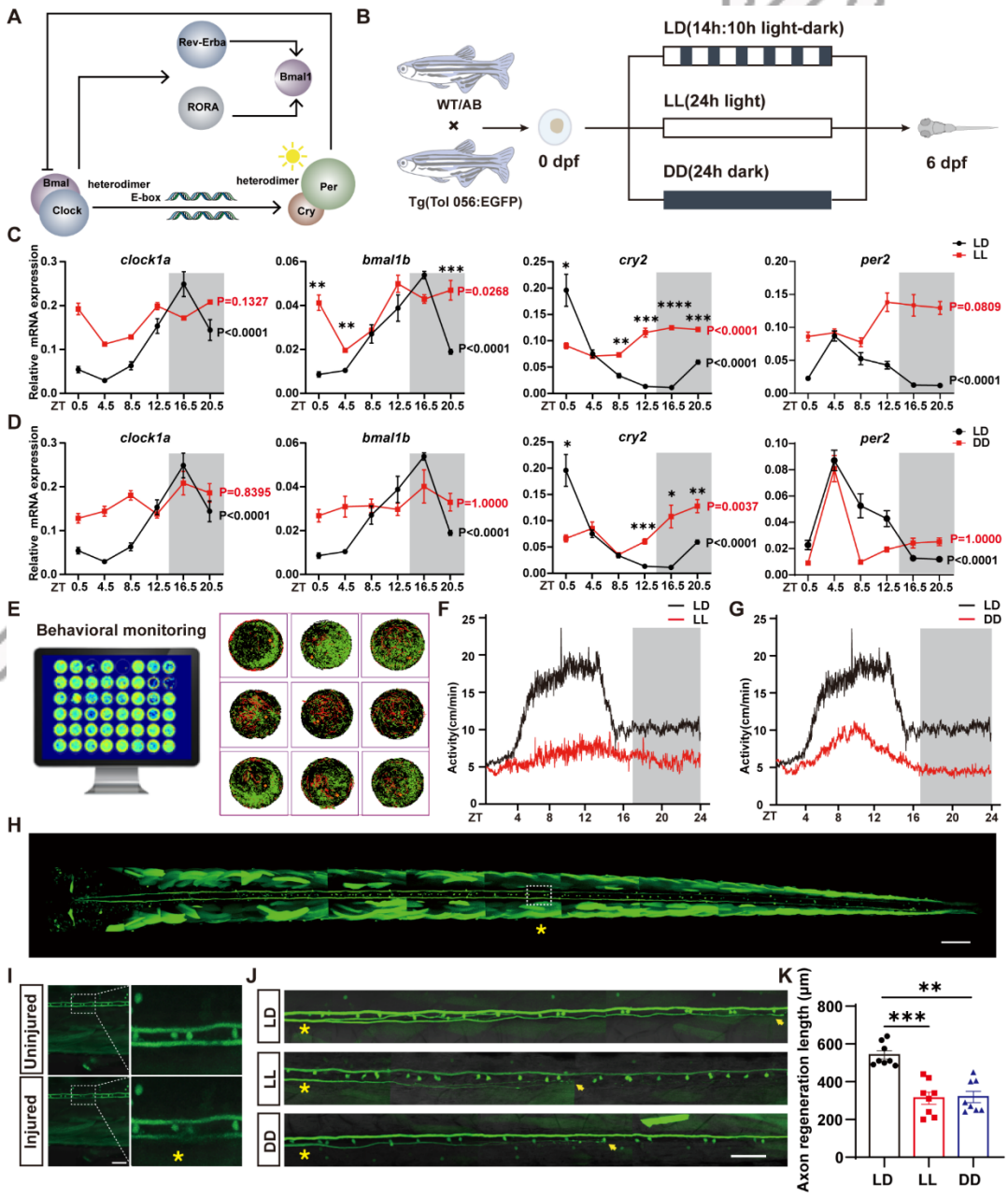

Figure 1. Circadian rhythm disruption impairs Mauthner cell axon regeneration

(A) The classical molecular feedback loop of the zebrafish circadian clock system. (B) Zebrafish embryos were raised under LD, DD, and LL conditions for 6 consecutive days. (C and D) Expression changes of core circadian clock genes in the circadian rhythm disruption model. pCycle values were calculated by Meta2d analysis adjusted for multiple comparisons. Two-way ANOVA was used to analyze the variation among different groups. Each experiment included three samples, and each sample contained 30 larvae. ZT, zeitgeber time; ZT0, light on; ZT14, light off. * $p < 0.05$, ** $p < 0.01$, *** $p < 0.001$, **** $p < 0.0001$ (E) The locomotion of larvae zebrafish was continuously monitored. (F and G) The locomotion of larvae raised under LL and DD conditions showed irregular rhythms compared to the control group ($n = 16$ larvae from 3 independent experiments). (H) Comprehensive view of EGFP-labeled cell bodies and axons of M-cells from the Tol-056 zebrafish strain. (I) Representative confocal images of an M-cell axons before and after ablation using a two-photon laser above the cloacal pore (Scale bar: 50 μm). (J and K) Compared to the LD group, the axon regeneration length of M cells in the LL and DD groups was significantly reduced. The yellow arrow indicates the distal end of the axon after 2 days of regeneration (Scale bar: 50 μm, $n = 8$ larvae from 3 independent experiments). All asterisks indicate the locations of injury sites. Data were analyzed with one-way ANOVA. ** $p < 0.01$, *** $p < 0.001$.

Circadian clock gene *per2* plays a crucial role in the zebrafish circadian system

Given that both continuous light and dark treatments disrupt circadian rhythms and result in the loss of circadian expression of the circadian clock gene *per2* **(Figure 1C, 1D)**. Furthermore, within the endogenous molecular clock of M cells, *per2* exhibits a relatively high expression level **(Figure S1D)**. Accordingly, *per2* was selected as the

first candidate gene to explore the intrinsic molecular mechanisms by which the circadian clock regulates axon regeneration in central neurons. First of all, the effectiveness of the *per2*$^{-/-}$ mutation was confirmed genetic testing and proteomic matching identification **(Figure S3A, S3B)**. Transcriptome analysis demonstrated that *per2*$^{-/-}$ mutations dysregulated the expression of regeneration-related genes, with the concomitant upregulation of inhibitors (e.g., *ptenb*, *socs3b*) (Jin et al., 2015) and downregulation of promoters (e.g., *gap43*, *mycb*) (Zhang et al., 2022) of axonal regeneration **(Figure S4A–S4C)**. As a core component of the circadian clock, Per2 plays a pivotal role in regulating critical physiological processes in mammals, including metabolism, development, and inflammatory responses in mice (Grimaldi et al., 2010; Bhatwadekar et al., 2013; Brenna et al., 2021; Guo et al., 2023). To evaluate its role in the circadian system of zebrafish, the expression of core clock genes and clock-controlled genes was quantified in the 6 dpf *per2*$^{-/-}$ mutants using quantitative PCR. The results revealed that *per2*$^{-/-}$ mutations significantly disrupted the expression of *per1b*, *per3*, *cry2*, and *aanat2*, consistent with previous studies **(Figure 2A)**(Wang et al., 2015a). Subsequently, to assess the reproductive and developmental effects of *per2*, embryo production, survival rate, and hatching rate were measured. Similar to findings in mammalian studies, our research found that the hatching and survival rates of zebrafish larvae were significantly reduced in the *per2*$^{-/-}$ mutations **(Figure 2B– 2D)**. Consistent with prior research, the locomotion distance of *per2*$^{-/-}$ mutants during the one-second light onset showed a significant decrease compared to that of the wild-type control in the visual motor response (VMR) assay **(Figure 2E, 2F)**(Huang et al., 2018). Although Per2 regulates sleep in mammals (Curie et al., 2015), its role in zebrafish sleep remains uninvestigated. We evaluated total sleep and locomotion activities over a complete light-dark cycle in both groups, finding a significant reduction

in overall movement distance in *per2*$^{-/-}$ mutants **(Figure 2G, 2H)**. Thus, these results highlight the essential role of *per2* in regulating circadian rhythms and associated physiological activities in zebrafish.

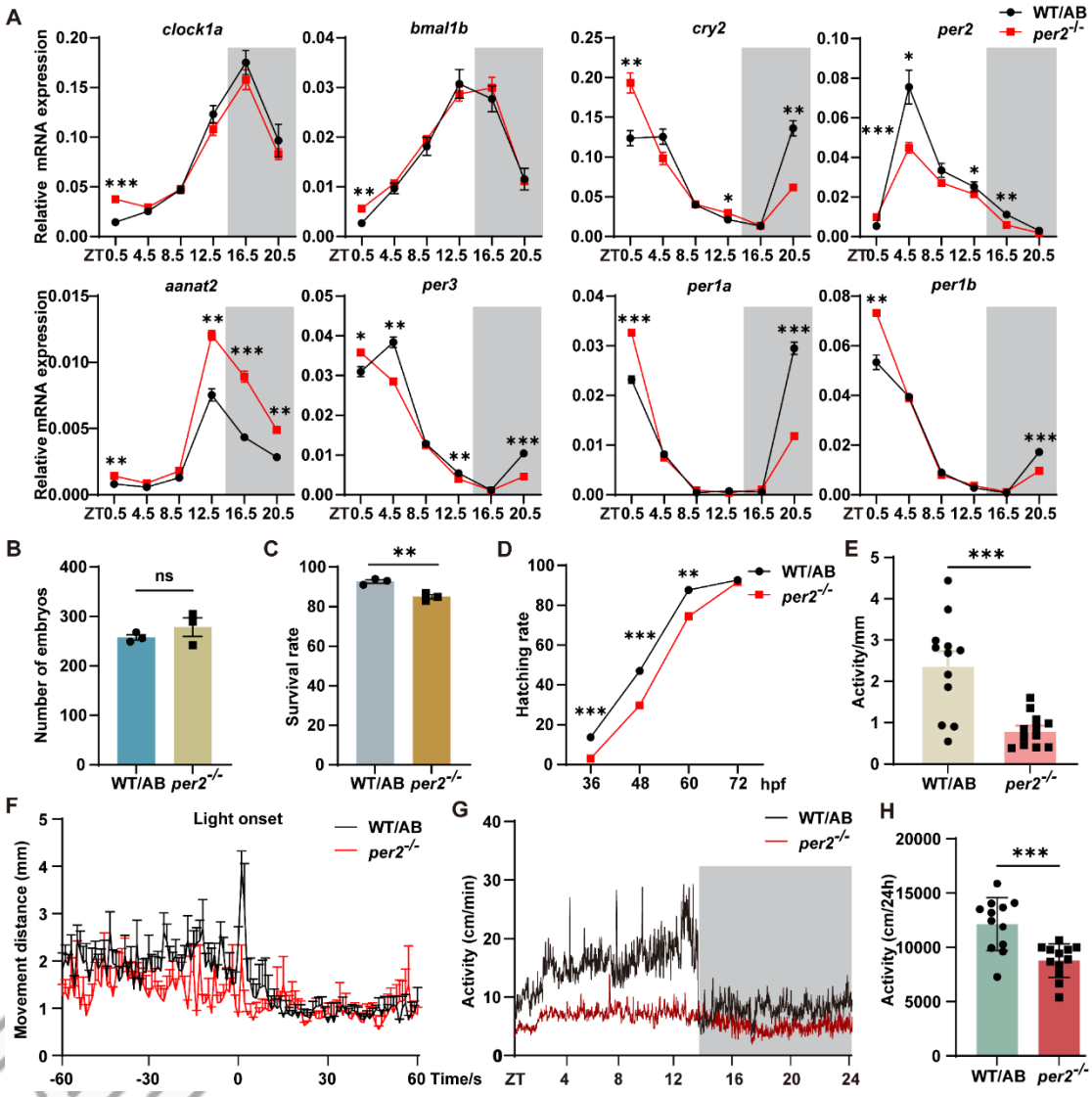

Figure 2. Circadian *per2* played a crucial role in the zebrafish clock

(A) Zebrafish embryos were raised in LD conditions for 6 consecutive days. Total RNA was extracted from WT and *per2*$^{-/-}$ mutant larvae at 4 h intervals for 24 h. qPCR analysis showed that the expression pattern of key circadian clock genes *cry2*, *per1b*, *per2*, and *per3* was changed in *per2*$^{-/-}$ mutant. (Each experiment included three samples, and each sample contained 30 larvae.) (B) The spawning quantity of each pair of male and female *per2* $^{-/-}$mutants showed no significant difference compared to that of

the WT. (C) The embryo survival rate of *per2*$^{-/-}$ mutants was significantly lower compared to that of the WT. (D) The hatching rate of *per2*$^{-/-}$ mutant embryos was significantly lower compared to the WT at 36 hours, 48 hours, and 60 hours post-fertilization. (E and F) After 30 minutes of dark adaptation, the locomotion distance of *per2*$^{-/-}$ mutants within one second after the onset of light was significantly reduced compared to that of the WT. (G and H) *per2*$^{-/-}$ mutant exhibited irregular rhythmic patterns in their locomotor behavior over a diurnal cycle, and their overall locomotor activity was weaker compared to that of the WT (n = 12, each group). ZT, zeitgeber time; ZT0, light on; ZT14, light off. Data were analyzed with unpaired t-tests. Bar graphs represent the mean ± SEM. * $p < 0.05$, ** $p < 0.01$, *** $p < 0.001$, ns, not significant.

Deficiency of circadian clock gene *per2* suppresses axonal regeneration and motor function recovery in M cells

To further investigate the molecular mechanisms underlying circadian rhythm regulation in axon regeneration, a homozygous *per2*$^{-/-}$ mutant zebrafish line, in which M cells are labelled, was generated by crossing the *per2*$^{-/-}$ mutants with the *Tg (Tol-056)* strain for two generations (**Figure 3A**). Additionally, the developmental body length at 6 dpf, the soma size of M cells, and the axon length from the cloaca to the tail in this *per2*$^{-/-}$ homozygous mutant line appeared normal (**Figure 3B–3E**). To assess the effects of the *per2*$^{-/-}$ mutation on axon regeneration, two-photon laser ablation of M cells axons was performed in both heterozygous and homozygous *per2*$^{-/-}$ mutants at 6 dpf. We photographed the regenerating axons and measured their lengths on 2 dpi **(Figure S3C and Figure 3E)**. The result showed a significant reduction in regenerated axon length of the M cells in both the heterozygous and homozygous *per2*$^{-/-}$ mu-

tants **(Figure S3E, S3F and Figure3F, 3G)**. To evaluate the impact of axon regeneration on zebrafish escape behavior, we conducted experiments focused on their escape responses. Zebrafish exhibit a rapid escape behavior in response to external acoustic stimuli or predators, primarily driven by M cells. The escape response includes two phases: the C-start, initiated by M cells, and the following escape swimming **(Video S2)**. Previous studies have shown a strong correlation between the M cells recovery and the C-start response (Liu and Hale, 2017). Given the significant reduction of axon regeneration length in *per2*$^{-/-}$ zebrafish. We aimed to assess the functional recovery of M cells via the escape response. Larval escape responses to acoustic stimuli were recorded using high-speed cameras **(Figure 3H, 3I)**. Analysis of the maximum turning angle and the time to reach this angle revealed no significant differences between the control and the *per2*$^{-/-}$ groups of intact axons **(Figure 3J, 3K)**. However, the injured *per2*$^{-/-}$group showed a significantly reduced maximum escape angle and a delay time to reach the angle compared to the control group at 2 dpi **(Figure 3L, 3M)**. These findings suggested that the functional recovery of the escape response, driven by M cells, was significantly impaired in *per2*$^{-/-}$ zebrafish.

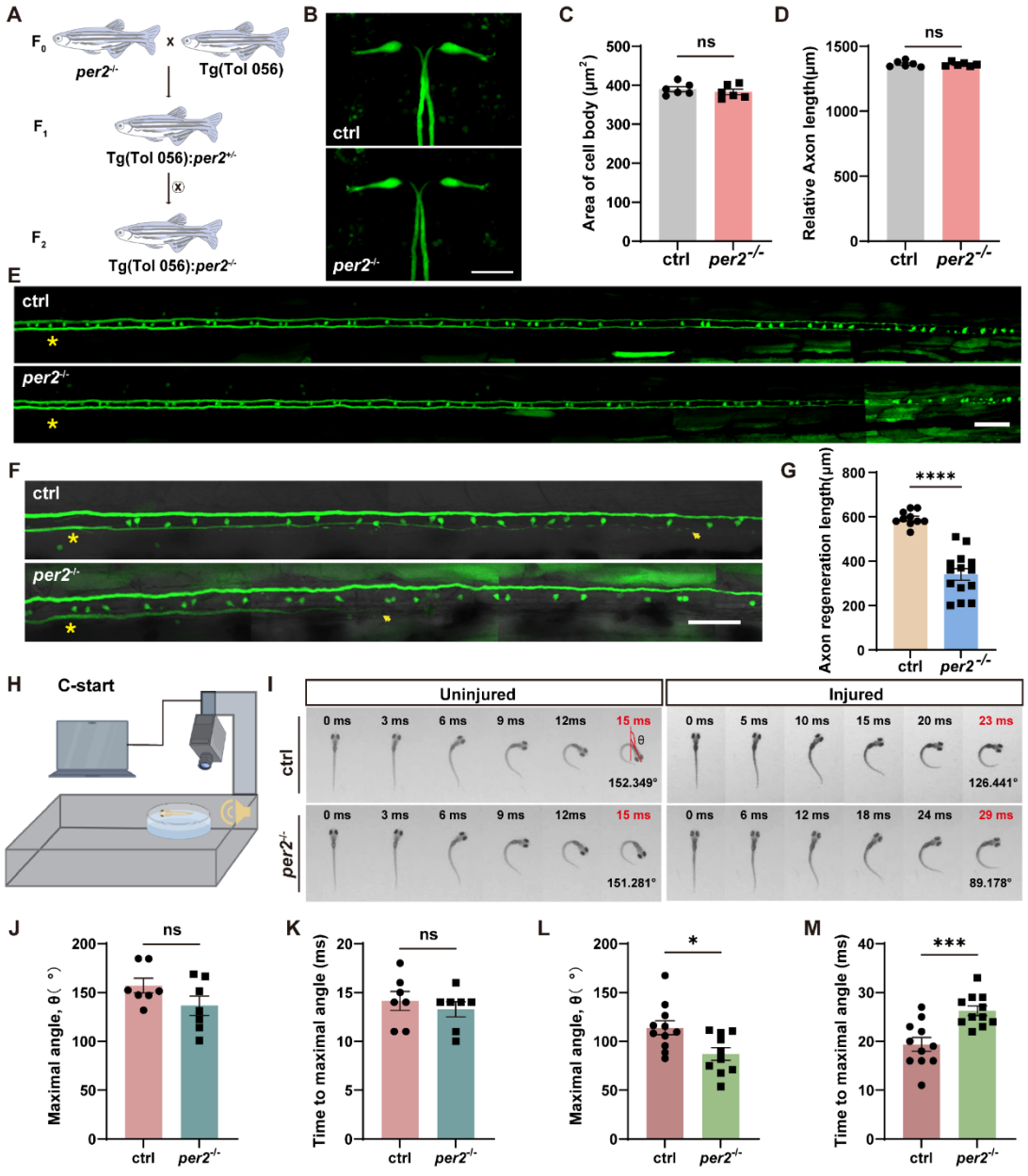

Figure 3. The *per2* mutation impairs the regeneration of Mauthner cell axons and the escape response mediated by them

(A) Hybridization of the transgenic line Tg (Tol-056) and *per2*$^{-/-}$ mutant was performed for two consecutive generations to obtain the Tg (Tol-056); *per2*$^{-/-}$ line. (B and C) The soma area of M cell in *per2*$^{-/-}$ mutant zebrafish did not show a significant difference compared to that of the control group at 6 dpf. (n = 6, each group, Scale bar: 50 μm). (D and E) The axonal length from the cloacal aperture to the end in 6 dpf *per2*$^{-/-}$ mutant zebrafish is comparable to that of the control group. (F and G) Confocal

imaging and quantification results showed that the axon regeneration length in *per2*$^{-/-}$ mutant zebrafish 2 dpi is significantly reduced compared to that of the control group. (H) The device for escape behavior tests. (I) Representative images showed the original orientation, maximal turn angle position, and the duration to reach the maximal turn angle in the uninjured and injured groups of control and *per2*$^{-/-}$ larvae zebrafish. Red lines indicate the heading direction. (J and K) Before axon injury, there was no significant difference in the maximal turn angle position and duration taken to reach the maximal turn angle. (L and M) After injury, the maximal turn angle of *per2*$^{-/-}$ mutants decreased, but duration taken to reach the maximal turn angle significantly increased. Data were analyzed with unpaired t-tests. Bar graphs represent the mean ± SEM. * $p < 0.05$, *** $p < 0.005$, **** $p < 0.001$, ns, not significant.

Transcriptome sequencing revealed the crucial role of *per2* in neural regeneration

Previous studies have showed that mutations in the *per2* gene significantly impaired zebrafish circadian rhythms, and sleep-wake cycles (Wang et al., 2015a). Here, Mauthner neuronal axon regeneration was also shown to be impaired in the *per2*$^{-/-}$ mutants. Nevertheless, the detailed molecular mechanisms underlying these functions within the circadian cycle remain inadequately characterized. Our investigation of a comprehensive 24-hour transcriptomic analysis comparing *per2*$^{-/-}$ mutants with control groups, revealed that the *per2*$^{-/-}$ mutation disrupted the circadian expression patterns of 3,193 genes (**Figure 4A, 4B**). Importantly, Gene Ontology (GO) analysis identified a significant enrichment in biological processes pivotal for axonal development and regeneration, including axonogenesis, neuronal differentiation, axon guid-

449 ance, axon extension, responses to injury, and axonal regeneration (**Figure 4C**). Fur-
450 thermore, KEGG pathway analysis showed substantial enrichment in neural regenera-
451 tion-associated pathways, such as the Wnt signaling pathway, oxidative phosphoryla-
452 tion, the tricarboxylic acid cycle, and autophagy (**Figure 4D**).
453
454 To identify genes of the most pronounced changes, we performed an intersection
455 analysis on genes that consistently showed both significant differential expression at
456 all six measured time points and arrhythmic expression patterns. This analysis yielded
457 several genes critical for neural regulation, including *carboxypeptidase E* (*cpe*), Bacu-
458 loviral IAP Repeat Containing 2 (*birc2*), FYVE, RhoGEF and PH Domain Containing
459 4a (*fgd4a*), casein kinase 1 Epsilon (*csnk1e*), aconitase 2 (*aco2*) and Rho/Rac Gua-
460 nine Nucleotide Exchange Factor 2 (*arhgef2*) (**Figure 4E, 4F**)(Fabrizi et al., 2009;
461 Cheng et al., 2013; Huang et al., 2015; Torii et al., 2023; Olivier et al., 2024). The
462 previously published transcriptomic dataset from a mammalian spinal cord injury
463 model (GSM1103369) was analyzed, revealing that *CPE* expression was significantly
464 downregulated at both 2 and 7days post-injury **(Figure S5A)**. In contrast, analysis of
465 a peripheral nerve regeneration dataset (GSE71453) showed a marked upregulation of
466 *CPE* following injury **(Figure S5B)**. These opposing expression patterns suggest that
467 elevated *CPE* levels may be a critical determinant for successful neuronal regenera-
468 tion. Further interactive analysis with single-cell transcriptomics of M cell before and
469 after axon injury revealed dramatic alterations in the expression of the neurotrophic
470 factor Cpe. An intersection analysis was conducted between the differentially ex-
471 pressed genes (DEGs) from Mauthner cell single-cell transcriptomics (Song et al.,
472 2025) and the circadian dysregulated genes (CDGs) obtained from circadian tran-

scriptomics **(Figure S5C)**. It was significantly upregulated in cases of successful regeneration and markedly downregulated in instances of failure, highlighting its potential regulatory role in axonal regeneration **(Figure S5D, S5E)**. CPE was initially recognized for its role in processing neuropeptides and peptide hormones (Hook et al., 1982). Beyond its enzymatic activity, CPE has been found to contribute to neuroprotection and neural development, thus earning the designation of neurotrophic factor-α1 (NFα1)(Cheng et al., 2013). Recent studies have shown that upregulating CPE can rescue hippocampal neurogenesis and memory deficits in aged mice with Alzheimer's disease(Jiang et al., 2024).

In conclusion, *cpe* was uniquely identified as a circadian-rhythmic and differentially expressed gene with regeneration enrichment, coupled with established functions in neuroprotection and growth. Its previously unexplored role in neural injury motivated our focus on its ability to promote axon regeneration.

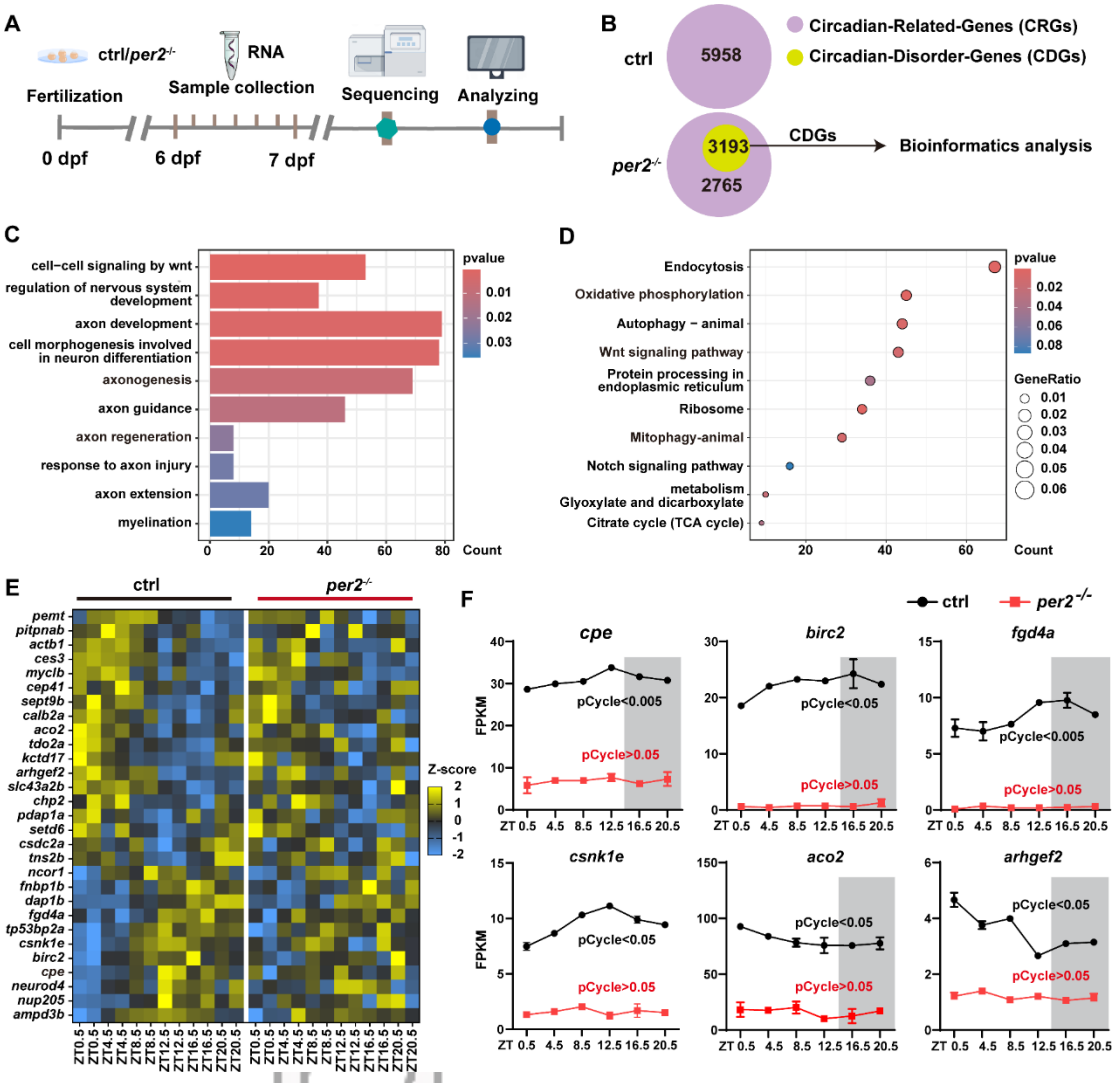

Figure 4. Circadian transcriptome sequencing revealed potential regulation of neural regeneration by the *per2* gene

(A)Timeline of time points of RNA extraction and RNA-seq. (B) The Venn diagram illustrated the CRGs (Circadian-Related-Genes, genes that exhibited significant rhythmic expression in WT zebrafish) and CDGs (Circadian-Disorder-Genes, genes that lost rhythmicity in the *per2*$^{-/-}$ mutants.) obtained from sequencing analysis of both the control and the *per2*$^{-/-}$ mutants. In the control group, there are 5,958 CRGs, while in the mutant strain, only 2,765 CRGs, among which 3,193 are CDGs. (C) The GO enrichment and enrichment for KEGG pathway analysis of CDGs. (D) The heatmap illustrated the most significantly circadian genes, with the control group on the left and

the *per2*$^{-/-}$ mutant group on the right. Samples were collected at ZT0.5, ZT4.5, ZT8.5, ZT12.5, ZT16.5, and ZT20.5 (6 time points, 2 independent experiments, each experiment included two samples, and each sample contained 30 larvae.). (F) The figure showed a subset of significantly altered circadian rhythm-disrupted genes. Transcripts of controls(black) are rhythmic (pCycle < 0.05 or pCycle < 0.005) while the *per2*$^{-/-}$ mutant (red) are out of rhythms. pCycle values were calculated by Meta2d analysis adjusted for multiple comparisons. ZT, zeitgeber time; ZT0, light on; ZT14, light off. Data were analyzed with unpaired *t*-tests. * $p < 0.05$ and ** $p < 0.01$.

The *per2* mutation and inhibition suppresses axonal regeneration via affecting the expression of *cpe*

To validate the alterations in Cpe expression in *per2*$^{-/-}$ mutant zebrafish, the expression of *cpe* throughout the day and its protein levels at ZT 12.5 and ZT 20.5 were examined with fluorescence PCR and Western blotting respectively. Our findings revealed a significant dysregulation and downregulation in *per2*$^{-/-}$ mutants, consistent with our transcriptomic data **(Figure 5A–5C)**. To explore the dose-dependent relationship between *per2* and *cpe*, we administered KL044, a Cryptochrome (Cry) stabilizer that indirectly suppresses Per2 activity by activating Cry protein, to larvae in varying concentrations (0.05, 0.2, and 0.5 μM) starting on 4 dpf (**Figure 5D**)(Lee et al., 2015) . After two days of treatment, axonal damage was induced at 6 dpf and the lengths of axon regeneration were measured on 2 dpi (**Figure 5G**). Our results showed that a concentration of 0.5 μM KL044 significantly curtailed the regeneration length of M cells (**Figure 5H**). Subsequent analysis of Cpe protein expression at this concentration showed significant downregulation compared to the DMSO control

group (**Figure 5E, 5F**). Collectively, these findings illuminated the role of the circadian gene *per2* in modulating axonal regeneration in zebrafish M cells through the regulatory control of the *cpe* expression.

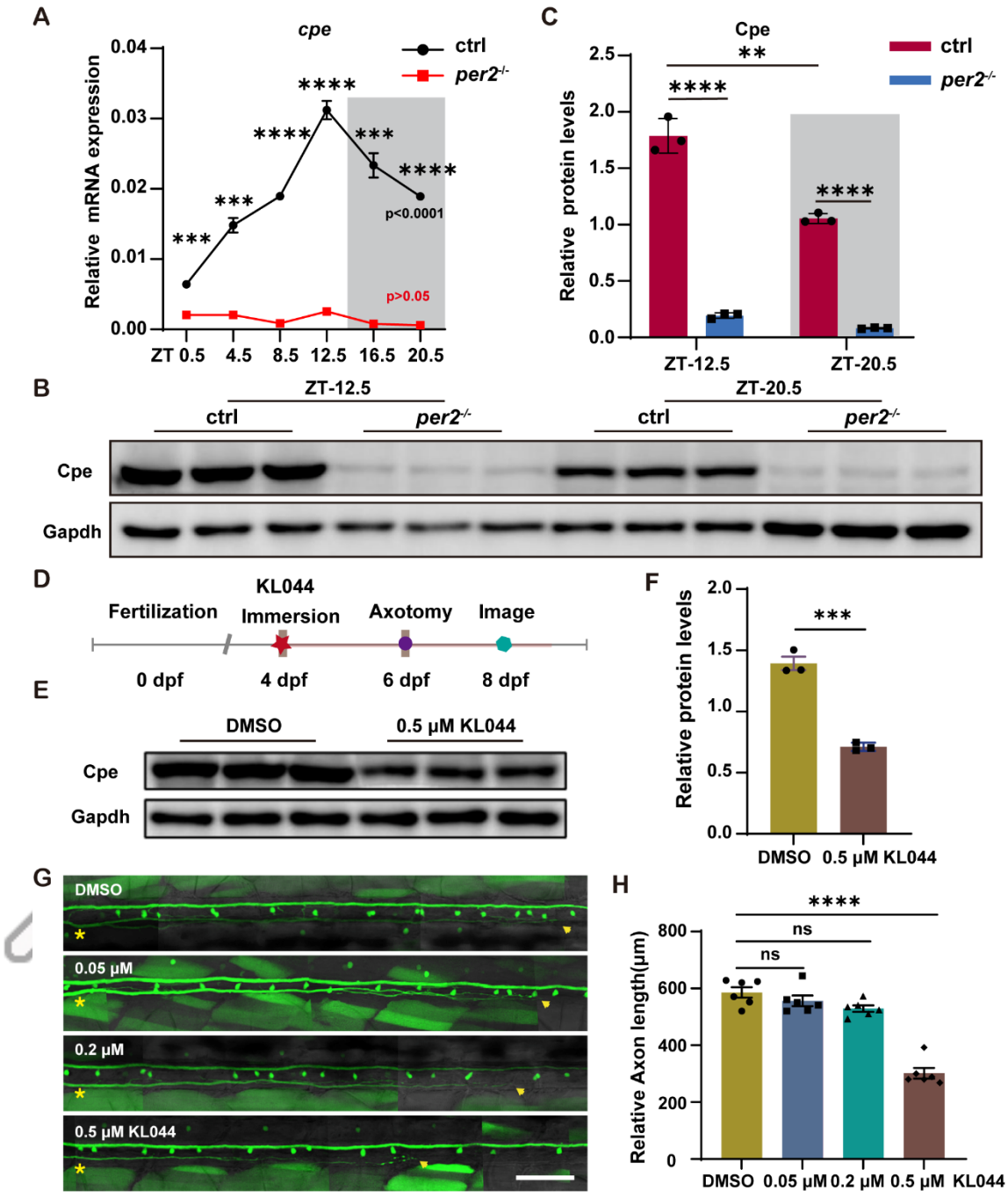

Figure 5. Per2 mutation and KL044 inhibition in regulating rhythmic expression and axon regeneration via Cpe protein in zebrafish

(A) C*pe* lost its rhythmic expression and was significantly downregulated in *per2*$^{-/-}$ mutants compared to the control group (Each experiment included three samples, and each sample contained 30 larvae). (B and C) In the control group, the expression of Cpe exhibited a circadian rhythm, being significantly higher at ZT12.5 compared to at ZT20.5. Additionally, at both ZT12.5 and ZT20.5, the expression levels were significantly higher than those in the *per2* mutants. (D) A flowchart exploring the regulation of axon regeneration by the Per2 protein inhibitor KL044. (F and G) Western blot and quantification results showed that treatment with 0.5 μM KL044 significantly reduced the protein expression levels of cpe. The bar graphs represent, the normalized expression values of *cpe* in the M-cells control group as well as in the regenerative and non-regenerative groups. (G) A representative diagram of confocal imaging of M-cells axon regeneration between DMSO and inhibitor (Concentration gradient, KL044: 0.05 μM, 0.2 μM, 0.5 μM). Asterisk: ablation site. Arrowhead, axon regeneration terminal; Scale bar, 50 μm. (H) Treatment with 0.5 μM KL044 significantly inhibited the axon regeneration of M cells (n = 6, each group). ZT, zeitgeber time; ZT0, light on; ZT14, light off. Data were analyzed with unpaired t-tests. ** $p < 0.01$, *** $p < 0.001$, **** $p < 0.0001$, ns, not significant.

Cpe knockdown suppresses the capacity of axon regeneration of M-cells

Subsequently, the impact of Cpe on axonal regeneration was investigated with pharmacological methods. Previous studies have indicated that 2-Guanidinoethylmercaptosuccinic acid (GEMSA) significantly inhibited enzymatic activity of the Cpe as a competitive inhibitor (Przewlocka et al., 1986). We treated 4 dpf larvae with 5 μM, 20 μM, and 50 μM of GEMSA to potentially reduce the Cpe activity, as previously described (Bommer et al., 1989). The effects of GEMSA on the *cpe* expression and

552 zebrafish development were evaluated. The results showed that GEMSA treatment
553 did not significantly affect zebrafish body length or Cpe protein expression levels dur-
554 ing the development (**Figure S6A-S6D**). Two days after the GEMSA treatment, ax-
555 onal injury was induced using two-photon laser ablation, and the lengths of axonal re-
556 generation were measured on 2 dpi (**Figure 6A**). The results demonstrated that sup-
557 pression of Cpe activity led to a significant reduction in the length of axonal regenera-
558 tion compared to that in the control group (**Figure 6B, 6C**).
559 To further clarify the regulatory role of *cpe* in M cells axon regeneration at the single-
560 cell level, we constructed pUAS-*miR30e-cpe* shRNA (1/2/3)-mCherry plasmids based
561 on a *miR-30e* backbone(Shen et al., 2024). An empty *miR-30e* plasmid was used as
562 control. These plasmids were co-injected with CMV-GAL4-VP16 into zebrafish em-
563 bryos at the 1-cell stage **(Figure 6D, 6E)**. All shRNA groups exhibited varying de-
564 grees of *cpe* knockdown, with shRNA1 showing the highest efficiency, reducing *cpe*
565 expression by more than 70% compared to the control group on 4 dpf **(Figure 6F)**.
566 These results confirmed the stability and sustained functionality of our miR-shRNA-
567 mediated knockdown system. Given its superior efficacy, shRNA1 was selected for
568 functional validation at the single-cell level. Using a single-cell electroporation plat-
569 form, shRNA1 was introduced into the M cells on one side of 4 dpf larvae. Two days
570 later, axonal injury was induced by two-photon laser ablation targeted above the cloa-
571 cal aperture on the electroporated side. Axon regeneration was subsequently assessed
572 at 2 dpi using confocal imaging **(Figure 6G)**. Quantitative analysis of axonal regener-
573 ation revealed a significant reduction in regrowth in *cpe*-deficient M cells compared
574 to controls **(Figures 6H, 6I)**, indicating that *cpe* knockdown impairs regenerative ca-
575 pacity at the single-cell level. Together with results from *per2*$^{-/-}$ mutant and KL044-

576 treated models, these findings suggested that both reduced *cpe* expression and sup-

577 pressed enzymatic activity compromise the intrinsic regenerative potential of

578 zebrafish M cells following axonal injury.

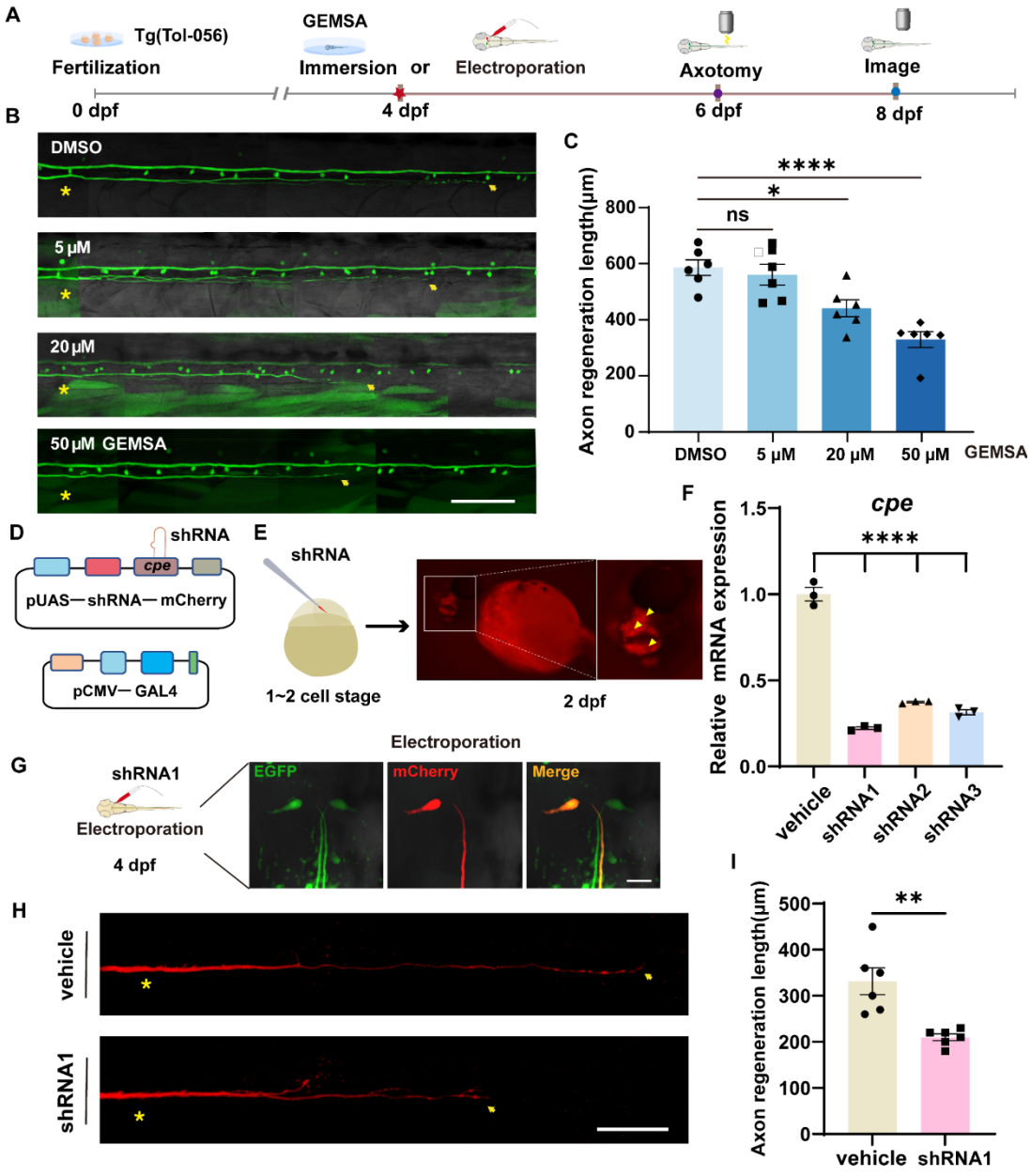

579

580 **Figure 6. Single-cell shRNA silencing of *cpe* inhibited axon regeneration in M**

581 **cells**

582 (A)Timing of inhibitor processing, electroporation, laser damage, and imaging. (B)

583 Representative diagram of confocal imaging of M-cells axon regeneration between

584 DMSO and GEMSA (Scale bar, 50 μm.) (C) Statistical quantitative diagram of axon

585 regeneration (n = 6, each group). Data shown as mean ± sem. Data were analyzed
586 with one-way ANOVA. * $p < 0.05$, **** $p < 0.0001$, ns, not significant. (D) Con-
587 struction of shRNA-*cpe* fusion expression plasmid. (E and F) Microinject the shRNA-
588 *cpe* plasmid into embryos at the 1-2 cell stage and assess the knockdown expression
589 of *cpe* in the positive larvae. Data were analyzed with one-way ANOVA. **** $p <$
590 0.0001. (G) Illustration of positively expressing larvae, where the most effective
591 shRNA1 for knockdown was electroporated into the M cells of 4 dpf larvae. (H) Rep-
592 resentative confocal images of M cells axon regeneration. (vehicle; shRNA1: *cpe*
593 knockdown, scale bar, 50 μm.). (I) Statistical quantification of axon regeneration (n =
594 6, each group). Data shown as mean ± sem. Data were analyzed with unpaired t-tests.
595 ** $p < 0.01$.
596
597 **Single-cell overexpression of *cpe* significantly enhances axon regeneration**
598 To determine whether *cpe* overexpression promotes M cells axon regeneration in the
599 zebrafish central nervous system, we constructed a plasmid-based overexpression sys-
600 tem. This system included CMV-GAL4-VP16/UAS-mCherry as the control and
601 CMV-GAL4-VP16/UAS-mCherry/UAS-*cpe* for the overexpression group **(Figure**
602 **S7A)**. To validate the efficiency and expression of the constructs, plasmids were mi-
603 croinjected into embryos at the 1-cell stage, followed by positive selection and qPCR
604 analysis on 2 dpf **(Figure S7B)**. The overexpression group exhibited a significant in-
605 crease in *cpe* transcript levels compared to the control **(Figure S7C).**
606 To assess the functional impact of *cpe* overexpression on axon regeneration, we em-
607 ployed the *Tg (Tol-056)* line, which specifically labels M cells. The overexpression
608 construct was electroporated into one M cells of 4 dpf larvae. Two days post-electro-

poration, axonal injury was induced via two-photon laser ablation, and axon regeneration was evaluated at 2 dpi using confocal imaging **(Figure 7A)**. Quantitative analysis revealed that *cpe* overexpression significantly enhanced axonal regeneration of M cells in the control group compared to those treated with the vehicle. Furthermore, when the *cpe* overexpression plasmid was introduced into M cells of *per2*$^{-/-}$ mutant larvae, axon regeneration was markedly improved relative to the vehicle-treated mutants **(Figure 7B, 7C)**. Escape responses were further evaluated across four experimental groups using the same behavioral paradigm **(Figure 7D)**. Prior to injury, all groups exhibited similar performance following acoustic stimulation, with no significant differences observed in maximum bending angle or escape latency **(Figure 7E, 7F)**. Baseline responses were not enhanced by *cpe* overexpression, likely due to a physiological ceiling effect of the fast-start reflex. Following injury, significant improvements in escape behavior were observed in the *cpe* overexpression group. In both the control and *per2*$^{-/-}$ mutant groups, increased escape angles and the reduced response times were recorded relative to the vehicle group **(Figure 7G, 7H)**. These findings demonstrated that Cpe functions as a potent neurotrophic factor that promotes axonal regeneration in zebrafish M cells, and highlight its conserved, pro-regenerative role in the vertebrate CNS *in vivo*.

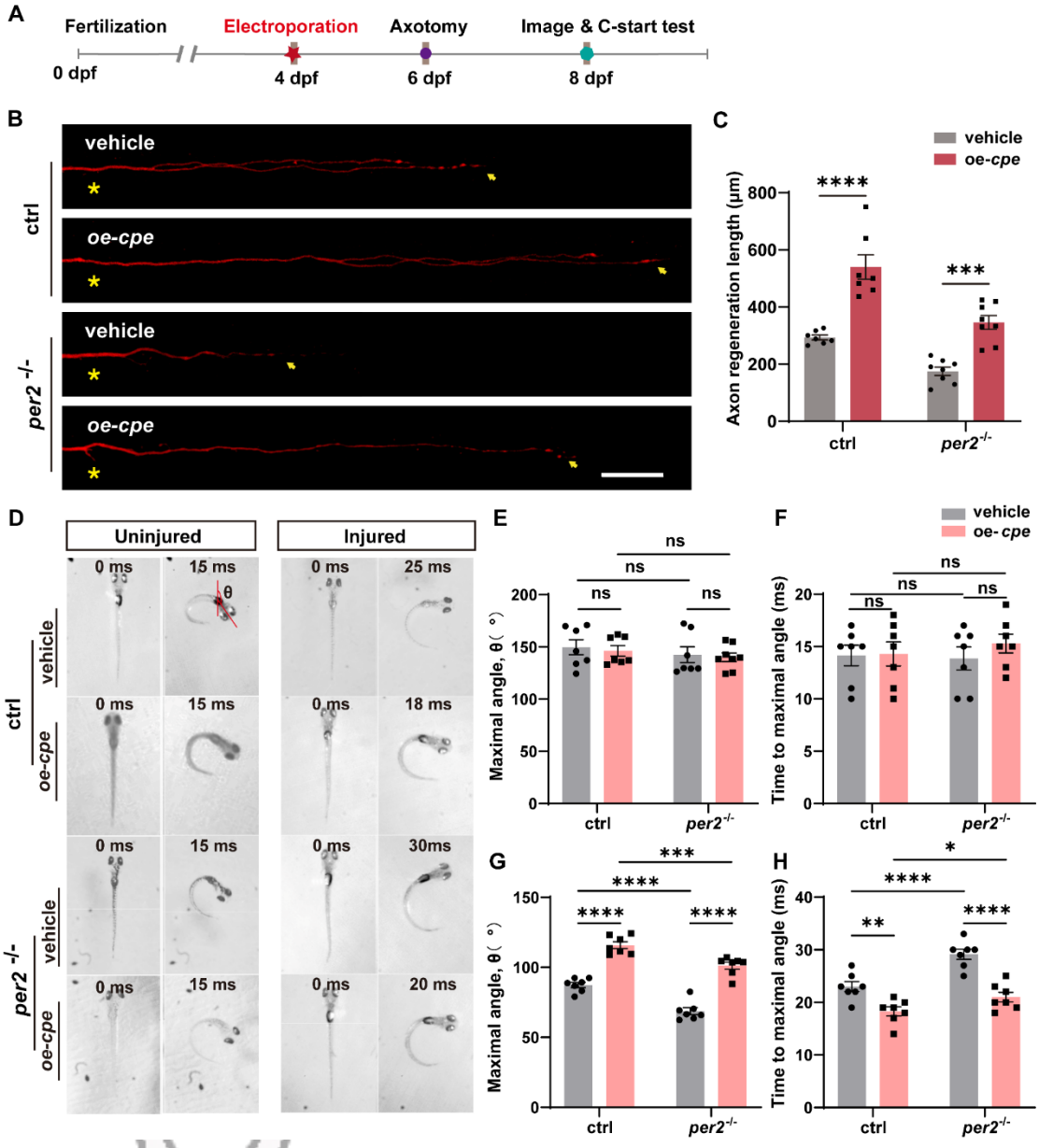

627

628 **Figure 7. Single-cell overexpression of *cpe* significantly promoted axon regenera-**

629 **tion and functional recovery in M cells**

630 (A) Timing of electroporation, laser damage, and imaging. (B) Representative confo-

631 cal images of M cells axon regeneration (Scale bar, 50 μm). (C) Statistical quantifica-

632 tion of axon regeneration (n = 7, each group in ctrl, n = 8, each group in *per2*$^{-/-}$). (D)

633 Representative images show the position of the maximum turning angle and the dura-

634 tion to reach it in larval zebrafish with uninjured and injured axons. (E and F) Before

635 axonal injury, the four groups of larval zebrafish showed no significant differences in

636 the position and duration to reach the maximum turning angle during escape re-
637 sponses (n = 7, each group). (G and H) *Cpe* overexpression in control and mutant
638 groups resulted in significantly larger deflection angles and reduced escape durations
639 (n = 7, each group). Data shown as mean ± sem. Data were analyzed with two-way
640 ANOVA. * $p < 0.05$, ** $p < 0.01$, **** $p < 0.0001$, ns, not significa
641
642 **DISCUSSION**
643 Here, we report the crucial role of circadian rhythms in regulating axon regeneration
644 in CNS neurons, based on the study of axon regeneration in zebrafish M cells. Our re-
645 search demonstrated that disruptions in the circadian rhythm, as well as via mutations
646 of *per2*, significantly impair the regenerative processes of axons. Previous studies
647 have highlighted the critical role of *per2* in regulating both the visual system and neu-
648 ronal synapses in zebrafish (Huang et al., 2018). Specifically, *per2* mutations lead to
649 abnormal development of the retinal synaptic layer, while experiments have directly
650 demonstrated that sleep pressure modulates synapse numbers at the level of individual
651 neurons (Suppermpool et al., 2024). Additionally, *per2* negatively regulates the ex-
652 pression of *aanat2*, a key gene in melatonin synthesis (Wang et al., 2015a). In mam-
653 mals, research has shown that depletion of either *Per1* or *Per2* inhibits myoblast dif-
654 ferentiation in vitro and impairs muscle regeneration *in vivo* (Katoku-Kikyo et al.,
655 2021). In Drosophila, circadian clock components modulate the regenerative state of
656 intestinal stem cells, rendering them more responsive to injury (Karpowicz et al.,
657 2013). Recent findings have also revealed that *Per2* activity aligns with the peak pe-
658 riod of macrophage-mediated clearance of β-amyloid, further underscoring its im-
659 portance in regulating neurological disorders (Song et al., 2015).

Nonetheless, the molecular mechanisms by which Per2 governs diverse physiological processes, particularly neural regeneration, remain poorly understood. Previous studies have shown the presence of an endogenous circadian clock in mouse sensory neurons, with axon regeneration and circadian clock-related genes exhibiting time-dependent enrichment throughout the day (De Virgiliis et al., 2023). It has also been discovered that the positive feedback regulator *Bmal1* gene plays a crucial role in peripheral nervous system regeneration, as *Bmal1* can epigenetically regulate axon regeneration in mouse sensory neurons (Halawani et al., 2023). However, the role of negative feedback factors *per* and *cry* in nerve regeneration has not yet been reported, nor has there been clear evidence of circadian clock regulation on central nervous system regeneration.

Zebrafish, as an ideal model for studying circadian rhythms, offer unique advantages (Frøland Steindal and Whitmore, 2019). Their circadian regulation mode is similar to that of humans, and their ability to respond directly to light makes research more convenient (Pando and Sassone-Corsi, 2002). By disrupting the zebrafish circadian clock through light manipulation, we discovered that circadian disruption does not affect the early development of central nervous system M cells but inhibits their axon regeneration capacity. This establishes a regulatory link between the circadian clock and central nervous system regeneration. We investigated the regulatory mechanism of the negative feedback factor *per2* gene on axon regeneration of M cells. Mutations or inhibition of *per2* impair axon regeneration of M cells and their mediated rapid escape response, further supplementing our understanding of circadian regulation of nervous system regeneration.

Our comprehensive transcriptomic analysis spanning the entire circadian cycle reveals a close association between the *per2* gene and the regulation of mitochondrial function, as well as the Wnt signaling pathway. Both of these molecular processes are essential for providing the energy required for repair mechanisms and for promoting the growth and guidance of new neurites. By integrating Mauthner cell single-cell transcriptomic data, we found that mutations in *per2* lead to the disruption and downregulation of the neurotrophic factor Cpe, which normally exhibits oscillatory expression in zebrafish with intact circadian rhythms.

In previous reports, Cpe known as NF-α1 not only differs from traditional neurotrophic factors BDNF, NGF, and GDNF in its receptor-mediated signaling mechanisms but also exhibits a unique dual functionality (Cheng et al., 2013; Park and Poo, 2013; Varadarajan et al., 2022). On the one hand, it participates in the processing and sorting of prohormones and proneuropeptides, thereby indirectly modulating the neurotrophic microenvironment through regulation of the maturation and secretion of dense-core vesicle contents (Cawley et al., 2012). On the other hand, as a secreted factor, Cpe can independently activate signaling pathways such as ERK–CREB to confer antioxidative and anti-apoptotic protection, while upregulating mitochondrial survival proteins like Bcl2 to support cellular energy metabolism, ultimately endowing it with the potential to promote neurogenesis as well as neuronal survival and regeneration following injury (Sharma et al., 2021). Overexpression of Cpe significantly increases neurogenesis in the mouse hippocampus and enhances the dendritic development of newborn neurons in vitro, effectively rescuing hippocampal neurogenesis and memory deficits associated with Alzheimer's disease (Jiang et al., 2024).

Previous studies have demonstrated that BDNF deficiency disrupts the intrinsic circadian rhythms in zebrafish, thereby highlighting the link between neurotrophic factors and the circadian clock (D'agostino et al., 2022). Importantly, our research shows that Per2 regulates the circadian oscillation of *cpe*, further integrating neurotrophic support with the molecular clock. These insights underscore the need for additional investigation of the Per2–Cpe regulatory axis and suggest that chronotherapeutic strategies exploiting this interaction could offer significant benefits for the treatment of neurodegenerative diseases. Our *in vivo* studies on *cpe* demonstrated that its reduction and activity inhibition hinder axon regeneration of zebrafish M cell, while overexpression of *cpe* significantly enhanced axon regeneration and effectively counters the damaging effects of circadian disruption. This further reveals the role of *cpe* not only in neuroprotection but also in its potential application value in promoting the repair of damaged neurons and enhancing their regenerative capacity. Furthermore, the disruption of *per2* leads to a notable decrease in the expression of the neurotrophic factor Cpe, which is possibly closely associated with reduced regenerative capacities. Next, our data confirmed that both the reduction and decreased activity of Cpe significantly inhibit the axonal regeneration of M-cells. Conversely, the overexpression of Cpe in individual cells markedly enhances the axonal regenerative capacity.

In conclusion, this study reveals the critical role of the circadian clock in CNS regeneration, highlighting the importance of circadian stability for axonal regeneration. It enhances our understanding of the effects of the circadian clock on CNS regeneration. The rhythmic expression of the neurotrophic factor *cpe* and the regulatory role of *per2* in Cpe provide new evidence for their potential as therapeutic targets for related dis-

eases. The compelling results of Cpe overexpression in augmenting axonal regeneration underscore the necessity for further research to explore and optimize the delivery mechanisms and efficacy of such interventions in clinical settings.

While our study provided significant insights, it is not without limitations. Zebrafish offer unique advantages for studying the circadian clock and possess remarkable regenerative abilities, making them favorable for researching central nervous system regeneration (Kyritsis et al., 2012; Zhang et al., 2025). However, they may not fully represent the physiological and genetic contexts of mammals, particularly humans. In mammals and humans, CNS injuries often struggle to regenerate and restore function due to intrinsic microenvironmental constraints and limited regenerative capacity. To advance understanding of Per2 and Cpe interactions, methodological investigations in phylogenetically advanced mammalian systems or human neuronal in vitro models are imperative to definitively characterize the neuroregenerative capacity of Cpe. While providing mechanistic insights through single-cell molecular perturbations effectively maps functional attributes of Cpe, such targeted methodologies restrict holistic analysis of its interactome dynamics and the multicomponent regulatory circuitry orchestrating neural tissue repair. Due to the current lack of established M cell-specific genetic manipulation tools and the technical challenges in constructing overexpression vectors for the large *per2* gene fragment, we were unable to perform M-cell-specific interventions for *per2* and instead utilized a systemic *per2*$^{-/-}$ model. Consequently, we cannot completely rule out the possibility that the observed regeneration defects are secondary to systemic circadian rhythm disruption. While our experiments

demonstrate the importance of stable *per2* expression for axon regeneration, developing M-cell-specific genetic manipulation models will be a key focus of our future research to ultimately clarify this issue.

Moreover, current research on the circadian clock's regulation in the nervous system is scarce, and studies focusing on individual genes like Per2 or Bmal1 struggle to elucidate the complexity of the broader circadian regulatory network, which involves multiple genes and feedback loops. Our current data mining and analysis of circadian transcriptomic sequencing represent only the tip of the iceberg. Future studies should conduct a more comprehensive and in-depth investigation into the broad physiological impacts of circadian rhythm disruption and *per2* gene mutations. Enhancing or inhibiting one or more circadian clock genes necessitates careful consideration and evaluation of potential physiological impacts. Research on the circadian clock requires overcoming the challenges of continuous day-night experiments, and we hope that future studies will increasingly focus on and invest in chronotherapy and research on neurological disorders.

Abbreviations

ANOVA: Analysis of variance

CNS: Central nervous system

dpf: Days post-fertilization

dpi: Days post-injury

DRG: Dorsal root ganglia

GO: Gene Ontology

KEGG: Kyoto Encyclopedia of Genes and Genomes

M cell: Mauthner cell

qRT-PCR: Quantitative Real-time PCR

SCI: Spinal cord injury

SEM: Standard error of the mean

WT: Wild-type

ZT: *Zeitgeber* time, ZT0 is defined as the time when lights are turned on in a controlled light-dark cycle.

ACKNOWLEDGMENTS

Thanks to the Core Facility Center for Life Sciences, University of Science and Technology of China. Thanks to Professor Wang Han (Soochow University, China), who provided the *per2*$^{-/-}$ knockout zebrafish line. Thanks to Shin-ichi Higashijima (RIkagaku KENkyusho/Institute of Physical, and Chemical Research, RIKEN), who provided the *Tg (Tol-056)* zebrafish strain with which M-cells were labeled by enhanced green fluorescent protein (EGFP). Thanks to the Revealer (Hefei, Anhui, China) for the help with the high-speed camera.

DATA AVAILABILITY

All data that support the findings of this study are available from the corresponding author upon reasonable request.

SUPPLEMENTARY DATA

Supplementary data to this article can be found online.

COMPETING INTERESTS

The authors declare that they have no competing interests.

AUTHORS' CONTRIBUTIONS

D. G. Fan, K. Q. Li, and B. Hu designed the research; D. G. Fan, J. H. Zhou, A. Han, and K. Q. Li performed the research; Z. A. Zhao, X. H. Tang, D. G. Fan, and K. Q. Li analyzed the data; Z. A. Zhao, X. H. Tang, Z. Song, D. G. Fan, and B. Hu wrote the paper.

All authors read and approved the final version of the manuscript.

REFERENCES

Allen SJ, Watson JJ, Shoemark DK, et al. 2013. GDNF, NGF and BDNF as therapeutic options for neurodegeneration. *Pharmacol Ther*, **138**(2): 155-175.

Appelbaum L, Wang GX, Maro GS, et al. 2009. Sleep-wake regulation and hypocretin-melatonin interaction in zebrafish. *Proceedings of the National Academy of Sciences of the United States of America*, **106**(51): 21942-21947.

Bhatwadekar AD, Yan Y, Qi X, et al. 2013. Per2 mutation recapitulates the vascular phenotype of diabetes in the retina and bone marrow. *Diabetes*, **62**(1): 273-282.

Bommer M, Nikolarakis K, Noble EP, et al. 1989. In vivo modulation of rat hypothalamic opioid peptide content by intracerebroventricular injection of guanidinoethylmercaptosuccinic acid (GEMSA): possible physiological role of enkephalin convertase. *Brain Res*, **492**(1-2): 305-313.

Brenna A, Ripperger JA, Saro G, et al. 2021. PER2 mediates CREB-dependent light induction of the clock gene Per1. *Sci Rep*, **11**(1): 21766.

Cawley NX, Wetsel WC, Murthy SR, et al. 2012. New roles of carboxypeptidase E in endocrine and neural function and cancer. *Endocr Rev*, **33**(2): 216-253.

Chen AQ, Xue M, Qiu CZ, et al. 2023. Circadian clock1a coordinates neutrophil recruitment via nfe212a/duox-reactive oxygen species pathway in zebrafish. *Cell Rep*, **42**(10): 113179.

Chen X, Shen Y, Song Z, et al. 2024. microRNA-2184 orchestrates Mauthner-cell axon regeneration in zebrafish via syt3 modulation. *J Genet Genomics*, **51**(9): 911-921.

Cheng Y, Cawley NX, Loh YP. 2013. Carboxypeptidase E/NFα1: a new neurotrophic factor against oxidative stress-induced apoptotic cell death mediated by ERK and PI3-K/AKT pathways. *PLoS One*, **8**(8): e71578.

Cooper JF, Guasp RJ, Arnold ML, et al. 2021. Stress increases in exopher-mediated neuronal extrusion require lipid biosynthesis, FGF, and EGF RAS/MAPK signaling. *Proceedings of the National Academy of Sciences of the United States of America*, **118**(36).

Cox J & Mann M. 2008. MaxQuant enables high peptide identification rates, individualized p.p.b.-range mass accuracies and proteome-wide protein quantification. *Nat Biotechnol*, **26**(12): 1367-1372.

Curie T, Maret S, Emmenegger Y, et al. 2015. In Vivo Imaging of the Central and Peripheral Effects of Sleep Deprivation and Suprachiasmatic Nuclei Lesion on PERIOD-2 Protein in Mice. *Sleep*, **38**(9): 1381-1394.

D'agostino Y, Frigato E, Noviello TMR, et al. 2022. Loss of circadian rhythmicity in bdnf knockout zebrafish larvae. *iScience*, **25**(4): 104054.

De Virgiliis F, Mueller F, Palmisano I, et al. 2023. The circadian clock time tunes axonal regeneration. *Cell Metab*, **35**(12): 2153-2164.e2154.
El Bejjani R & Hammarlund M. 2012. Notch signaling inhibits axon regeneration. *Neuron*, **73**(2): 268-278.
Fabrizi GM, Taioli F, Cavallaro T, et al. 2009. Further evidence that mutations in FGD4/frabin cause Charcot-Marie-Tooth disease type 4H. *Neurology*, **72**(13): 1160-1164.
Fontana X, Hristova M, Da Costa C, et al. 2012. c-Jun in Schwann cells promotes axonal regeneration and motoneuron survival via paracrine signaling. *J Cell Biol*, **198**(1): 127-141.
Frøland Steindal IA & Whitmore D. 2019. Circadian Clocks in Fish-What Have We Learned so far? *Biology (Basel)*, **8**(1).
Grimaldi B, Bellet MM, Katada S, et al. 2010. PER2 controls lipid metabolism by direct regulation of PPARγ. *Cell Metab*, **12**(5): 509-520.
Guo L, Cen H, Weng J, et al. 2023. PER2 integrates circadian disruption and pituitary tumorigenesis. *Theranostics*, **13**(8): 2657-2672.
Halawani D, Wang Y, Ramakrishnan A, et al. 2023. Circadian clock regulator Bmal1 gates axon regeneration via Tet3 epigenetics in mouse sensory neurons. *Nat Commun*, **14**(1): 5165.
Hecker A, Anger P, Braaker PN, et al. 2020. High-resolution mapping of injury-site dependent functional recovery in a single axon in zebrafish. *Commun Biol*, **3**(1): 307.
Hook VY, Eiden LE, Brownstein MJ. 1982. A carboxypeptidase processing enzyme for enkephalin precursors. *Nature*, **295**(5847): 341-342.
Hu BB, Chen M, Huang RC, et al. 2018. In vivo imaging of Mauthner axon regeneration, remyelination and synapses re-establishment after laser axotomy in zebrafish larvae. *Exp Neurol*, **300**: 67-73.
Huang DF, Wang MY, Yin W, et al. 2018. Zebrafish Lacking Circadian Gene per2 Exhibit Visual Function Deficiency. *Front Behav Neurosci*, **12**: 53.
Huang G, Zhang F, Ye Q, et al. 2016. The circadian clock regulates autophagy directly through the nuclear hormone receptor Nr1d1/Rev-erbα and indirectly via Cebpb/(C/ebpβ) in zebrafish. *Autophagy*, **12**(8): 1292-1309.
Huang LG, Li JP, Pang XM, et al. 2015. MicroRNA-29c Correlates with Neuroprotection Induced by FNS by Targeting Both Birc2 and Bak1 in Rat Brain after Stroke. *CNS Neurosci Ther*, **21**(6): 496-503.
Jiang D, Liu H, Li T, et al. 2024. Agomirs upregulating carboxypeptidase E expression rescue hippocampal neurogenesis and memory deficits in Alzheimer's disease. *Transl Neurodegener*, **13**(1): 24.
Jin D, Liu Y, Sun F, et al. 2015. Restoration of skilled locomotion by sprouting corticospinal axons induced by co-deletion of PTEN and SOCS3. *Nat Commun*, **6**: 8074.
Karpowicz P, Zhang Y, Hogenesch JB, et al. 2013. The circadian clock gates the intestinal stem cell regenerative state. *Cell Rep*, **3**(4): 996-1004.
Katoku-Kikyo N, Paatela E, Houtz DL, et al. 2021. Per1/Per2-Igf2 axis-mediated circadian regulation of myogenic differentiation. *J Cell Biol*, **220**(7).
Korn H & Faber DS. 2005. The Mauthner cell half a century later: a neurobiological model for decision-making? *Neuron*, **47**(1): 13-28.
Krylov VV, Izvekov EI, Pavlova VV, et al. 2021. Circadian rhythms in zebrafish (Danio rerio) behaviour and the sources of their variability. *Biol Rev Camb Philos Soc*, **96**(3): 785-797.

Kyritsis N, Kizil C, Zocher S, et al. 2012. Acute inflammation initiates the regenerative response in the adult zebrafish brain. *Science*, **338**(6112): 1353-1356.
Lane JM, Qian J, Mignot E, et al. 2023. Genetics of circadian rhythms and sleep in human health and disease. *Nat Rev Genet*, **24**(1): 4-20.
Lee JW, Hirota T, Kumar A, et al. 2015. Development of Small-Molecule Cryptochrome Stabilizer Derivatives as Modulators of the Circadian Clock. *ChemMedChem*, **10**(9): 1489-1497.
Liu YC & Hale ME. 2017. Local Spinal Cord Circuits and Bilateral Mauthner Cell Activity Function Together to Drive Alternative Startle Behaviors. *Curr Biol*, **27**(5): 697-704.
Olivier JF, Langlais D, Jeyakumar T, et al. 2024. CCDC88B interacts with RASAL3 and ARHGEF2 and regulates dendritic cell function in neuroinflammation and colitis. *Commun Biol*, **7**(1): 77.
Pando MP & Sassone-Corsi P. 2002. Unraveling the mechanisms of the vertebrate circadian clock: zebrafish may light the way. *Bioessays*, **24**(5): 419-426.
Park H & Poo MM. 2013. Neurotrophin regulation of neural circuit development and function. *Nat Rev Neurosci*, **14**(1): 7-23.
Parker SJ, Rost H, Rosenberger G, et al. 2015. Identification of a Set of Conserved Eukaryotic Internal Retention Time Standards for Data-independent Acquisition Mass Spectrometry. *Mol Cell Proteomics*, **14**(10): 2800-2813.
Patrón LA & Zinsmaier KE. 2016. Mitochondria on the Road to Power Axonal Regeneration. *Neuron*, **92**(6): 1152-1154.
Przewlocka B, Dziedzicka M, Silberring J, et al. 1986. Analgesic and convulsant effects of guanidinoethylmercaptosuccinic acid (GEMSA)--a potent enkephalin convertase inhibitor. *Neuropeptides*, **8**(4): 359-365.
Qin S, Zou Y, Zhang CL. 2013. Cross-talk between KLF4 and STAT3 regulates axon regeneration. *Nat Commun*, **4**: 2633.
Ruan W, Yuan X, Eltzschig H. 2021a. Circadian Mechanisms in Medicine. *N Engl J Med*, **384**(20): e76.
Ruan W, Yuan X, Eltzschig HK. 2021b. Circadian rhythm as a therapeutic target. *Nat Rev Drug Discov*, **20**(4): 287-307.
Sanges D, Romo N, Simonte G, et al. 2013. Wnt/β-catenin signaling triggers neuron reprogramming and regeneration in the mouse retina. *Cell Rep*, **4**(2): 271-286.
Sharma VK, Yang X, Kim SK, et al. 2021. Novel interaction between neurotrophic factor-α1/carboxypeptidase E and serotonin receptor, 5-HTR1E, protects human neurons against oxidative/neuroexcitotoxic stress via β-arrestin/ERK signaling. *Cell Mol Life Sci*, **79**(1): 24.
Shen Y, Chen X, Song Z, et al. 2024. MicroRNA-9 promotes axon regeneration of mauthner-cell in zebrafish via her6/ calcium activity pathway. *Cell Mol Life Sci*, **81**(1): 104.
Sillar KT. 2009. Mauthner cells. *Curr Biol*, **19**(9): R353-355.
Song H, Moon M, Choe HK, et al. 2015. Aβ-induced degradation of BMAL1 and CBP leads to circadian rhythm disruption in Alzheimer's disease. *Mol Neurodegener*, **10**: 13.
Song Z, Zhu L, Shen Y, et al. 2025. High-Quality Cell Capture Reveals Transcriptomic Changes After Single-Axon Injury of Mauthner Cells. *bioRxiv*: 2025.2003.2017.643681.
Suppermpool A, Lyons DG, Broom E, et al. 2024. Sleep pressure modulates single-neuron synapse number in zebrafish. *Nature*, **629**(8012): 639-645.

Terenzio M, Koley S, Samra N, et al. 2018. Locally translated mTOR controls axonal local translation in nerve injury. *Science*, **359**(6382): 1416-1421.
Torii S, Arakawa S, Sato S, et al. 2023. Involvement of casein kinase 1 epsilon/delta (Csnk1e/d) in the pathogenesis of familial Parkinson's disease caused by CHCHD2. *EMBO Mol Med*, **15**(9): e17451.
Varadarajan SG, Hunyara JL, Hamilton NR, et al. 2022. Central nervous system regeneration. *Cell*, **185**(1): 77-94.
Wang M, Zhong Z, Zhong Y, et al. 2015a. The zebrafish period2 protein positively regulates the circadian clock through mediation of retinoic acid receptor (RAR)-related orphan receptor α (Rorα). *J Biol Chem*, **290**(7): 4367-4382.
Wang Z, Reynolds A, Kirry A, et al. 2015b. Overexpression of Sox11 promotes corticospinal tract regeneration after spinal injury while interfering with functional recovery. *J Neurosci*, **35**(7): 3139-3145.
Wang Z, Wang X, Shi L, et al. 2022. Wolfram syndrome 1b mutation suppresses Mauthner-cell axon regeneration via ER stress signal pathway. *Acta Neuropathol Commun*, **10**(1): 184.
Wehner D, Tsarouchas TM, Michael A, et al. 2017. Wnt signaling controls pro-regenerative Collagen XII in functional spinal cord regeneration in zebrafish. *Nat Commun*, **8**(1): 126.
Xiao L, Chang SY, Xiong ZG, et al. 2017. Absence of Carboxypeptidase E/Neurotrophic Factor-A1 in Knock-Out Mice Leads to Dysfunction of BDNF-TRKB Signaling in Hippocampus. *J Mol Neurosci*, **62**(1): 79-87.
Zhai J, Kim H, Han SB, et al. 2021. Co-targeting myelin inhibitors and CSPGs markedly enhances regeneration of GDNF-stimulated, but not conditioning-lesioned, sensory axons into the spinal cord. *Elife*, **10**.
Zhang HY, Li KY, Wang YL, et al. 2025. ROS regulates circadian rhythms by modulating Ezh2 interactions with clock proteins. *Redox Biol*, **81**: 103526.
Zhang Y, Xu L, Li X, et al. 2022. Deciphering the dynamic niches and regeneration-associated transcriptional program of motoneurons following peripheral nerve injury. *iScience*, **25**(9): 104917.
Zheng B & Tuszynski MH. 2023. Regulation of axonal regeneration after mammalian spinal cord injury. *Nat Rev Mol Cell Biol*, **24**(6): 396-413.

昼夜节律 *per2* 通过羧肽酶 E 调节斑马鱼中枢神经元 毛特纳（Mauthner）细胞轴突再生

作者：凡定刚、李可强、赵子昂、周俊晖、唐夏会、韩阿龙、宋政

通讯作者：胡兵

IHM前沿交叉科学与生物医学研究所，合肥国家微尺度物质科学研究中心，生命科学与医学部，中国科学技术大学，合肥230026

摘要

中枢神经系统 （CNS） 损伤通常会导致永久性神经损伤或致命后果。虽然昼夜节律调节是影响周围神经元再生能力的关键途径，但内在生物钟在中枢神经系统轴突再生中的作用仍然难以捉摸。使用昼夜节律紊乱的斑马鱼幼鱼模型，我们观察到中枢神经系统单个毛特纳细胞（M 细胞）的轴突再生受到显着抑制。斑马鱼幼鱼中核心生物钟基因 *per2* 的突变或抑制严重损害了轴突再生和声学诱发的逃逸运动。一天中时间依赖性转录组学分析表明，*per2* 调节参与再生相关途径的基因，例如线粒体代谢和 Wnt 信号转导。此外，定量RT-PCR和蛋白质印迹实验表明，神经营养因子羧肽酶E（Cpe）在野生型中表现出强大的昼夜节律性，但在*per2*$^{-/-}$突变体中显着下调。Cpe 缺乏显著抑制轴突再生，而其过表达增强了再生能力，从而挽救了*per2*$^{-/-}$突变体的轴突再生损伤。总体而言，我们的研究结果证明了稳定的昼夜节律系统和 *per2* 在中枢神经系统再生中的关键作用，以及 Cpe 在促进轴突再生方面的潜在功能。

关键词：生物钟、轴突再生、斑马鱼、毛特纳细胞